Computations of Intermittent Transport in Scrape-Off Layer Plasmas

O. E. Garcia, V. Naulin, A. H. Nielsen, and J. Juul Rasmussen
Association EURATOM-Risø National Laboratory, OPL-128 Risø, DK-4000 Roskilde, Denmark
(Received 2 September 2003; published 21 April 2004)

Two-dimensional fluid simulations of interchange turbulence for geometry and parameters relevant for the scrape-off layer of magnetized plasmas are presented. The computations, which have distinct plasma production and loss regions, reveal bursty ejection of particles and heat from the bulk plasma in the form of blobs. These structures propagate far into the scrape-off layer where they are dissipated due to transport along open magnetic field lines. From single-point recordings it is shown that the blobs have asymmetric conditional wave forms and lead to positively skewed and flattened probability distribution functions. The radial propagation velocity may reach one-tenth of the sound speed. These results are in excellent agreement with recent experimental measurements.

DOI: 10.1103/PhysRevLett.92.165003 PACS numbers: 52.35.Ra, 52.25.Gj, 52.55.Dy, 52.65.Kj

Recently, several experimental investigations have revealed a strongly intermittent nature of particle and heat transport in the scrape-off layer (SOL) of magnetized plasmas [1–3]. There are strong indications that this is caused by field-aligned structures in the form of plasma blobs propagating radially far into the SOL. It has been suggested that this is due to the dipole vorticity field caused by vertical guiding center motions in nonuniformly magnetized plasmas [4]. An outstanding challenge is to give a self-consistent description of the emergence and evolution of such structures, which also captures their statistical properties. Here an attempt towards this goal is presented, yielding favorable agreement with experimental measurements. This is achieved by focusing on the collective two-dimensional dynamics perpendicular to the magnetic field while using a simplified description of particle and heat losses along open field lines.

Some of the most prominent features of experimental single-point measurements are asymmetric conditional wave forms as well as positively skewed and flattened probability distribution functions (PDFs) of the density and temperature signals [1–3]. Simple interpretations as well as advanced imaging techniques give a picture of field-aligned blobs or filaments propagating out of the bulk plasma with radial velocities up to one-tenth of the sound speed c_s. These highly nonlinear thermal structures have amplitudes that significantly exceed the background levels. A change of sign in the asymmetry of the fluctuation time series close to the last closed flux surface (LCFS) indicates that the structures are generated by a local relaxation of the edge pressure profile [1]. This leads to an ejection of blobs of excess particles and heat into the SOL, where the structures are subject to parallel losses. This separation of driving and damping regions in configuration space has been discarded in previous simulations of SOL turbulence [5,6]. On the other hand, while three-dimensional computations include most of the detailed geometry and physics, they are restricted to small integration times and are usually run with frozen profiles [7].

In this Letter we present a novel model for interchange turbulence in slab geometry and numerical solutions in qualitative agreement with experimental measurements. The model geometry comprises distinct plasma production and loss regions, corresponding to the inner edge and SOL of magnetized plasmas. The separation of these two regions defines an effective LCFS, though we do not include magnetic shear in our model. In the edge region, large pressure gradients maintain a state of turbulent convection. However, a self-regulation mechanism involving differential rotation leads to repetitive expulsions of hot plasma into the SOL, resulting in asymmetric conditional wave forms and PDFs, and significant cross-field transport by the turbulent structures.

Assuming cold ions and neglecting electron inertia effects, a three-field model may be derived for quasineutral electrostatic perturbations of the full particle density $n(\mathbf{x}, t)$, electron temperature $T(\mathbf{x}, t)$, and electric potential $\phi(\mathbf{x}, t)$. Using the Bohm normalization and slab coordinates with $\hat{\mathbf{z}}$ along the magnetic field we obtain [8]

$$\frac{dn}{dt} + nC(\phi) - C(nT) = \nu_n \nabla^2 n - \sigma_n (n-1) + S_n,$$

$$\left(\frac{\partial}{\partial t} + \hat{\mathbf{z}} \times \nabla\phi \cdot \nabla\right)\Omega - C(nT) = \nu_\Omega \nabla^2 \Omega - \sigma_\Omega \Omega,$$

$$\frac{dT}{dt} + \frac{2T}{3} C(\phi) - \frac{7T}{3} C(T) - \frac{2T^2}{3n} C(n) = \nu_T \nabla^2 T - \sigma_T (T-1) + S_T,$$

where the vorticity is given by $\Omega = \nabla_\perp^2 \phi$, time is normalized by the ion gyration period, $1/\omega_{ci}$, and spatial scales are

 © 2004 The American Physical Society

given by the hybrid gyration radius, $\rho_s = c_s/\omega_{ci}$. The particle density n and temperature T are normalized to fixed characteristic values at the outer wall. We further define the two-dimensional advective derivative and the magnetic field curvature operator,

$$\frac{d}{dt} = \frac{\partial}{\partial t} + \frac{1}{B}\hat{\mathbf{z}} \times \nabla\phi \cdot \nabla, \qquad C = \nabla\left(\frac{1}{B}\right)\cdot\hat{\mathbf{z}} \times \nabla,$$

respectively, where $B(x) = 1/(1 + \varepsilon + \zeta x)$ is the toroidal magnetic field, $\varepsilon = a/R_0$ the inverse aspect ratio, and $\zeta = \rho_s/R_0$. The terms on the right hand side of the model equations describe external sources S, collisional diffusion with coefficients ν, and damping of all fields at rate σ. The latter is a simplified representation of parallel losses due to end sheaths in regions of open magnetic field lines. As the turbulent time scale is comparable with the loss time scale, the blobs are extended along the magnetic field lines but have a nontrivial parallel structure. Thus, the local parallel loss of particles and charge from a blob need not be directly connected with the overall losses at the sheaths. This is different from the standard two-dimensional sheath dissipation model [4,5]. The validity of either of these models may be questioned. However, we again emphasize that our main focus is on the nonlinear collective dynamics. The geometry and boundary conditions are sketched in Fig. 1.

In the absence of external sources and dissipative processes the model equations nonlinearly conserve particles as well as the global energy

$$E(t) = \int d\mathbf{x}\left[\frac{1}{2}(\nabla_\perp\phi)^2 + \frac{3}{2}nT\right],$$

where the integral extends over the whole plasma layer. Thus, the curvature terms correctly yield a conservative energy transfer from the confined heat to the convective motions. We further define the kinetic energy of the fluctuating and mean motions,

$$K(t) = \int d\mathbf{x}\frac{1}{2}(\nabla_\perp\tilde{\phi})^2, \qquad U(t) = \int d\mathbf{x}\frac{1}{2}v_0^2, \quad (1)$$

where the zero index denotes an average over the periodic direction y and the spatial fluctuation about this mean is indicated by a tilde. The linearly damped mean flow, $v_0(x,t) = \partial\phi_0/\partial x$, does not yield any radial convective transport and hence forms a benign path for fluctuation energy. The energy transfer rates from thermal energy to the fluctuating motions, and from the fluctuating to the mean motions, are given, respectively, by

$$F_p(t) = \int d\mathbf{x}nTC(\phi), \qquad F_v(t) = \int d\mathbf{x}\tilde{v}_x\tilde{v}_y\frac{\partial v_0}{\partial x}. \quad (2)$$

Note that F_p is essentially a measure of the domain integrated convective thermal energy transport, while F_v shows that structures tilted to transport positive poloidal momentum up the gradient of a sheared flow sustain the mean flow against dissipation [9].

In the following we present results from a numerical simulation of the interchange model using parameters relevant for SOL plasmas. The dimensions of the simulation domain are $L_x = 2L_y = 400$, and the LCFS is located at $x_{\mathrm{LCFS}} = 100$. The parameters are $\varepsilon = 0.25$, $\zeta = 10^{-3}$, and $\nu = 5 \times 10^{-3}$ is taken to be the same for all fields. The parallel loss rate of temperature is assumed to be 5 times larger than that of density and vorticity, $\sigma_n = \sigma_\Omega = \sigma_T/5 = \zeta/2\pi q$, since primarily hot electrons are lost along open field lines. Here σ_n and σ_Ω are estimated as the loss rate over one connection length $2\pi qR_0$ with the acoustic speed c_s, where $q = 3$ is the safety factor at the edge. Finally, the radial line integral of the sources S_n and S_T equals 0.2, and the shape of the sources and parallel loss coefficients shown in Fig. 1 are given by $\delta = 16$ and $\xi = 2$. The numerical solution has spatial resolution of 512 and 256 grid points in the radial and poloidal directions, respectively. The time span of the simulation is 4×10^6.

In Fig. 2 we show the typical evolution of the particle confinement P and heat confinement H in the edge and SOL regions, defined by

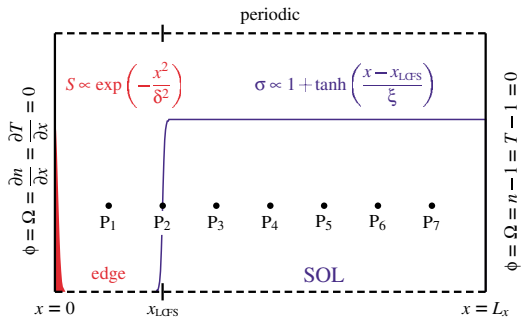

FIG. 1 (color online). Geometry of the simulation domain showing the forcing region to the left, corresponding to the edge plasma, and the parallel loss region to the right, corresponding to the scrape-off layer. Data time series are collected at the probe positions P_i.

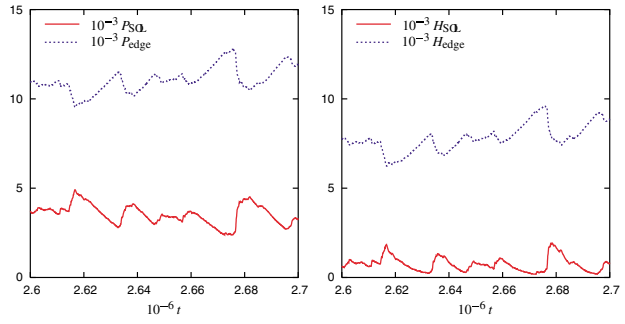

FIG. 2 (color online). Evolution of particle confinement P and the heat confinement H in the edge and scrape-off layer regions, showing sawtoothlike oscillations.

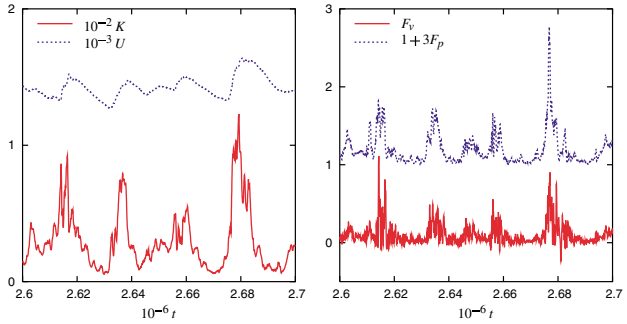

FIG. 3 (color online). Evolution of the kinetic energies and the collective energy transfer terms, showing bursty behavior in the fluctuation integrals.

$$P_{\text{edge}}(t) = \int_0^{x_{\text{LCFS}}} dx n_0(x,t),$$

$$P_{\text{SOL}}(t) = \int_{x_{\text{LCFS}}}^{L_x} dx n_0(x,t),$$

and similarly for the heat confinement H being the integral of temperature. From the figure we observe that plasma and heat gradually builds up in the edge at the same time as it is decaying in the SOL region. This is repetitively interrupted by rapid changes in which plasma and heat is lost from the edge to the SOL. More than 20% of the edge plasma may be lost during individual bursts. Also note from the figure that the normalized heat confinement is much less than the particle confinement due to the larger loss rate in the SOL region of the former. Further insight is revealed by Fig. 3, which shows the evolution of the kinetic energy contained by the fluctuating and mean motions [confer Eq. (1)], as well as the energy transfer terms defined in Eq. (2). From this figure we observe that the convective energy and thermal transport appear as bursts during which particles and heat are lost from the edge into the SOL region. As discussed in Ref. [9], such global dynamics is caused by a self-regulation mechanism in which kinetic energy is transferred from the fluctuating to the mean motions, and

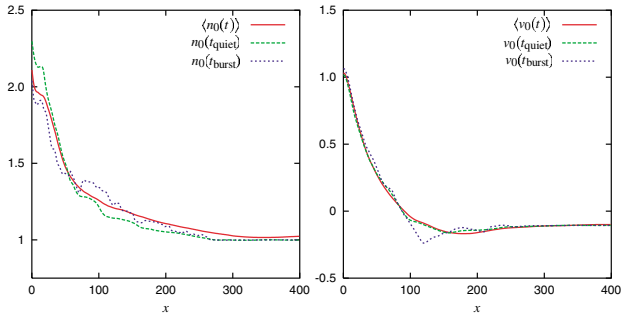

FIG. 4 (color online). Time-averaged profiles of plasma particle density n_0 and mean poloidal flow v_0, and typical profiles during a fluctuation burst and during a quiet period.

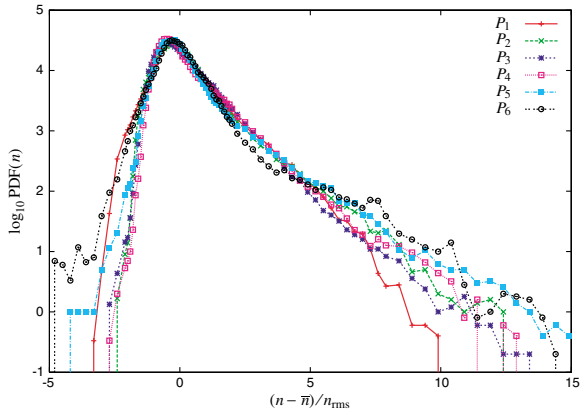

FIG. 5 (color online). Probability distribution functions of particle density measured at different radial positions P_i as shown in Fig. 1. The vertical axis shows count numbers.

subsequently damped by collisional dissipation. As the particle and heat confinement is allowed to vary, this results in the sawtoothlike oscillations seen in Fig. 2 [9].

The time-averaged profiles of the particle density and the mean poloidal flows are shown in Fig. 4. Parallel losses in the SOL region result in steep average profiles inside the LCFS and weakly decaying throughout the SOL. Also shown in Fig. 4 are typical instantaneous profiles during a quiet period (t_{quiet}) and during a burst (t_{burst}). We observe significant deviations from the average profiles, with a more peaked particle density profile in the edge region during quiet phases. During the turbulent phase there is a substantial particle increase in the SOL region due to the convective plasma transport. It is also seen that there is larger flow amplitudes during bursts due to the efficient energy transfer from tilted convection cells; confer Fig. 3.

The statistics of single-point recordings at different radial positions P_i indicated in Fig. 1 agrees very well with experimental measurements. In Fig. 5 we present the

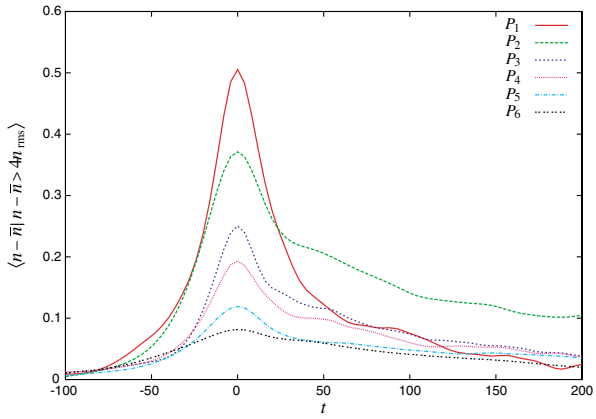

FIG. 6 (color online). Conditionally averaged wave forms of the particle density measured at different radial positions P_i as shown in Fig. 1, using the local condition $n-\overline{n} > 4n_{\text{rms}}$.

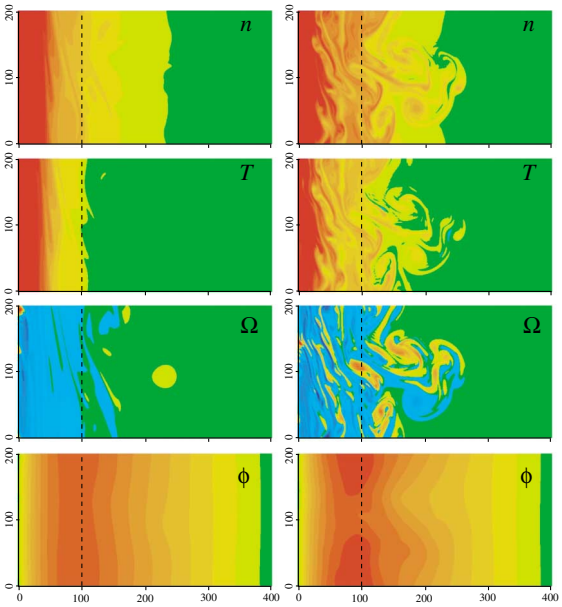

FIG. 7 (color online). Typical spatial structure of density, temperature, vorticity, and electric potential during a quiet period to the left and during a burst to the right. The broken vertical lines indicate the last closed flux surface.

PDFs of the density signals taken from a long-run simulation containing more than a hundred burst events. The positively skewed and flattened distributions indicate a high probability of large positive fluctuations corresponding to blobs of excess plasma. At all points the PDFs have a similar structure with a pronounced exponential tail towards large values. The skewness and flatness factors take values up to 3 and 15, respectively. The conditionally averaged temporal wave forms calculated from the same signals, using the local trigger condition $n - \overline{n} > 4n_{\mathrm{rms}}$ where $\overline{n}$ is the time-averaged density, are presented in Fig. 6. An asymmetric wave form with a sharp rise and a relatively slow decay is clearly seen [1–3]. The maximum density excursions significantly exceed the background level, and decay rapidly as the structures propagate through the SOL. The number of realizations for the conditional averaging decreases gradually from 125 at the innermost probe to 2 at the outermost one. We thus ignore the last probe in the statistical analysis. By following the evolution of individual structures we find that their radial propagation velocity is close to one-tenth of the sound speed but with a large statistical variance, again in agreement with experimental measurements.

Finally, in Fig. 7 we show the spatial structure of the density, temperature, vorticity, and electrostatic potential during a quiet period and during a burst. These correspond to the same times as the instantaneous profiles shown in Fig. 4. In the quiet period there are only weak spatial fluctuations with the plasma and heat well confined within the LCFS. In the turbulent phase bloblike structures are clearly observed for the density and temperature fields. These structures have propagated far into the SOL and are naturally associated with strong vorticity [4,9].

In this Letter we have proposed a new model for interchange turbulence and demonstrated that it has numerical solutions in good agreement with measurements reported from experimental investigations of SOL turbulence and intermittent transport events [1–3]. The formation and radial propagation of hot plasma blob structures is, indeed, associated with local relaxations of the plasma pressure profile, leading to skewed conditional wave forms and probability distributions. As emphasis is put on the collective dynamics, the qualitative aspects of these results are likely to be persistent with respect to changes in model geometry and underlying instability mechanisms. A more complete description of plasma transport in SOL plasmas requires long-run and well-resolved three-dimensional global simulations with appropriate geometry and boundary conditions, as well as allowing profile relaxations.

This work was supported by the Danish Center for Scientific Computing through Grants No. CPU-1101-08 and No. CPU-1002-17. O. E. G. has been supported by financial subvention from the Research Council of Norway.

[1] J. A. Boedo *et al.*, J. Nucl. Mater. **313–316**, 813 (2003); Phys. Plasmas **10**, 1670 (2003); **8**, 4826 (2001); D. L. Rudakov *et al.*, Plasma Phys. Controlled Fusion **44**, 717 (2002).

[2] G. Y. Antar *et al.*, Phys. Plasmas **10**, 419 (2003); **8**, 1612 (2001); Phys. Rev. Lett. **87**, 065001 (2001).

[3] J. L. Terry *et al.*, Phys. Plasmas **10**, 1739 (2003); S. J. Zweben *et al.*, *ibid.* **9**, 1981 (2002); R. J. Maqueda *et al.*, *ibid.* **8**, 931 (2001).

[4] S. I. Krasheninnikov, Phys. Lett. A **283**, 368 (2001); D. A. D'Ippolito *et al.*, Phys. Plasmas **9**, 222 (2002); N. Bian *et al.*, *ibid.* **10**, 671 (2003).

[5] Y. Sarazin *et al.*, J. Nucl. Mater. **313–316**, 796 (2003); Y. Sarazin and Ph. Ghendrih, Phys. Plasmas **5**, 4214 (1998).

[6] S. Benkadda *et al.*, Contrib. Plasma Phys. **34**, 247 (1994); O. Pogutse *et al.*, Plasma Phys. Controlled Fusion **36**, 1963 (1994).

[7] X. Q. Xu *et al.*, New J. Phys. **4**, 53 (2002); Nucl. Fusion **42**, 21 (2002); J. Nucl. Mater. **266–269**, 993 (1999).

[8] A derivation of the model will be presented in an extended report. See, however, V. Naulin *et al.*, Phys. Lett. A **321**, 355 (2004) and O. E. Garcia, J. Plasma Phys. **65**, 81 (2001).

[9] N. H. Bian and O. E. Garcia, Phys. Plasmas **10**, 4696 (2003); V. Naulin *et al.*, *ibid.* **10**, 1075 (2003); O. E. Garcia and N. H. Bian, Phys. Rev. E **68**, 047301 (2003); O. E. Garcia *et al.*, Plasma Phys. Controlled Fusion **45**, 919 (2003).